Supplementary Information for

Novel insights into the charge storage mechanism in pseudocapacitive vanadium nitride thick films for high-performance on-chip micro-supercapacitors

Kevin Robert[1,2], Didier Stiévenard[1], Dominique Deresmes[1], Camille Douard[2,3], Antonella Iadecola[2], David Troadec[1], Pardis Simon[4], Nicolas Nuns[4], Maya Marinova[4], Marielle Huvé[4], Pascal Roussel[4], Thierry Brousse[2,3*] and Christophe Lethien[1,2*]

Correspondence to: **christophe.lethien@univ-lille.fr** & **thierry.brousse@univ-nantes.fr**

This PDF file includes the Materials and Methods sections, the supplementary Text, the additional figures S1 to S7 and the captions for the movies.

Other Supplementary Materials for this manuscript include the following movie S1.

Materials and Methods

Sputtering deposition of vanadium nitride (VN) film

Prior to the VN deposition, a Si_3N_4 layer (300 nm-thick) was deposited by a low-pressure chemical vapor deposition method (LPCD) at 800 °C (flow rates: 60 sccm for NH_3 and 20 sccm for SiH_2Cl_2) to protect the silicon wafer from the etching of the liquid electrolyte (1M KOH). VN films were prepared by DC-reactive magnetron sputtering of a pure 4" vanadium target (99.9 %) in an Alliance Concept CT200 reactor. Before the deposition, the pressure was kept below 10^{-6} mbar and the target-substrate distance was fixed at 6 cm. The pressure, power density, argon and nitrogen flow rates were fixed, respectively, at 7.5 x 10^{-3} mbar, 2 W cm^{-2}, 25 sccm and 5 sccm. The temperature was modified so as to tune the specific surface of the VN films, and different thicknesses were attained depending on the deposition time. To determine the composition of the films, 100 nm-thick VN films were prepared, based on the proposed deposition parameters, at 350 °C. 1 µm-thick VN films at 350 °C were used to investige the charge storage mechanism by X-Ray Absorption Spectroscopy at the *Soleil* synchrotron (Rock Beam line).

Fabrication of the VN / VN interdigitated micro-supercapacitors

Following the deposition of the Si_3N_4 (300 nm-thick) and VN layers by LP CVD, and their respective, a photoresist etching mask was spin coated on these nitride thin films. The Inductively Coupled Plasma Reactive Ion Etching (ICP RIE) process, based on chlorine/argon gases (Cl_2/Ar), was optimized to etch the VN layer selectively to the photoresist. To provide a good electrical isolation between the two interdigitated VN electrodes, the etching process was stopped once the first ten nanometers of the Si_3N_4 layer was etched. 40 micro-supercapacitors (MSCs) were

fabricated on a single silicon wafer (7.5 cm diameter / thickness = 0.385 mm) using this four-step process.

Structural and morphological characterizations of the VN thin films

To this end, the VN thin films were deposited on a high-resistivity silicon wafer (R > 5000 ohm.cm). Electrical measurements were performed by Foucault current using Semilab WT 2000PVN contactless equipment. TEM measurements were conducted on a S/TEM FEI TITAN Themis 300 equipped with a probe corrector for a resolution of 0.6 Å in STEM mode, an electron monochromator for an energy resolution of 140 meV, and a Super-X quad EDS detector for elemental analysis. The microscope has several annual detectors for imaging, and a post-column GATAN Quantum ERS/966 GIF operating a dual EELS mode.

For the STEM experiment, a spot-size 9, a convergence semi-angle of 20.5 mrad and a beam current of between 50 and 100 nA were used along with a HAADF detector collection angle of between 50 mrad and 200 mrad. The STEM-EELS experiment was performed in spectrum imaging mode with a dispersion of 0.25 eV/ch, 1.5 nm step and a 0.05 s dwell time, thereby simultaneously acquiring the low-loss and core-loss energy range and the collection angle, respectively, at 49 mrad. The spectrum images were later realigned to compensate for drift in energy by the zero-loss peak. The 7 µm-thick sputtered vanadium film was analyzed. Prior to this, the sample had been thinned and mounted on a TEM copper grid using a FIB / SEM technique, so as to meet the requirements for TEM observation.

A Zeiss Ultra 55 scanning electron microscope (SEM), an atomic force microscope (AFM Dimension 3100) and a microbalance from Mettler Toledo XP6U were used to determine the

morphology (cross section and top view analyses) of the films (thickness, roughness and density).

Structural properties were examined by X-ray diffraction using a Rigaku Smarlab diffractometer in Bragg-Brentano mode employing Cu Kα-radiation (λ = 1.5418 Å). An offset of 2° was applied on the silicon substrate to avoid the high intensity of the (100) silicon peak.

To determine the composition of the thin film along its thickness, ToF-SIMS paired with XPS measurement was performed. ToF-SIMS analyses were carried out using a TOF.SIMS^5 (IONTOF GmbH Germany) instrument equipped with a Bi^+ liquid metal ion gun (LMIG). Pulsed Bi^+ primary ions were used for the analysis (25 KeV, 1 pA), in negative detection and high current bunch modes. Sputtering was performed with a raster of 400 x 400 μm^2 using Cs^+ (1 keV, 75 nA). A bismuth beam was rastered over an area of 100 x 100 μm^2 with a pixel number of 128 x 128. In order to compensate for charges induced by the primary ion beam and sputter gun, a low-energy (20 eV) pulsed electron flood gun was used.

The sample was then transferred, under ultra-high vacuum (< 5.10^{-9} Torr), into the XPS analysis chamber. The surface area analyzed on the sample was 110 µm × 110 µm, centered on the sputter gun crater. The X-ray photoelectron spectroscopy (XPS) experiments were carried out in a Kratos AXIS Ultra DLD spectrometer using monochromatic Al Kα radiation (1486.6 eV) operating at 225 W. The instrument work function was calibrated to provide an Au $4f_{7/2}$ metallic gold binding energy (BE) of 83.95 eV. The spectrometer dispersion was adjusted to supply a binding energy of 932.63 eV for metallic Cu $2p_{3/2}$. High-resolution spectra were collected using a 20 eV pass energy. Instrument base pressure was 4×10^{-10} Torr. The V *2p*, O *1s*, N *1s* and C *1s* spectra were analyzed using CasaXPS software (version 2.3.16, Casa Software Ltd.). Spectra decomposition and

quantification were performed, subsequent to using a Shirley-type background subtraction and Gaussian–Lorentzian profiles with 70/30 Gaussian/Lorentzian proportion.

Operando X-Ray Absorption Spectroscopy at the V-K edge

Synchrotron X-ray absorption spectroscopy (XAS) was performed at a Vanadium K-edge energy in fluorescence mode at the ROCK beamline [1] of the SOLEIL synchrotron (Saint-Aubin, France). A channel-cut Si(111) Quick Exafs monochromator with an oscillating frequency of 0.5 Hz at the V K-edge was used to select the energy of the incident photons, and their intensity was measured using an ionization chamber. The fluorescence photons were collected using a Passivated Implanted Planar Silicon (PIPS, Canberra) as the detector, with a large active area (30 cm^2). A tailor-made three-electrode *in situ – operando* liquid cell was placed at 45 degrees with respect to the incident beam and the fluorescence detector (**Figure S3**). A sandwich of Kapton foil (0.01 mm) and PTFE (0.01 mm) was used as a transparent window for X-rays, in order to avoid leaks and to prevent beam radiation damage. Prior to performing the *operando* experiment, several tests were done to maximize the signal-to-noise-ratio of the XAS spectra as a function of the electrolyte concentration and the thickness of the VN films, using two cells with different optical paths (**Figure S4**). To avoid strong absorption, which occurs due to the high X-ray absorption coefficient of the electrolyte at 5500 eV, we used the cell with an 80 μm optical path and diluted the KOH concentration to 0.5 M. VN films with thicknesses ranging from 340 nm to 1 μm were deposited on a Si substrate, which was coated with Si_3N_4 (300 nm-thick) to avoid electrolyte corrosion. Due to the high penetration depth of the incident X-ray, several Bragg peaks of the Si substrate were observed in the XAS spectra, but simply rotating the cell slightly served to remove

them from the XANES region. The *operando* XAS experiment was performed on a 1 µm-thick film of VN electrode cycled between -0.4 V and -1.0 V vs Hg/HgO at 2 mV s^{-1}, using Pt as the counter electrode. No bubble formation was observed during the *operando* measurements. The 1st cycle did not include a XAS experiment perspective because the open-circuit potential of VN material is - 0.35 V vs Hg/HgO, which is outside of the electrochemical windows used (-1 up to -0.4 V vs Hg/HgO): we thus waited for 1st cycle to stabilize before performing the *operando* XAS analysis. For each cycle corresponding to 10 minutes of acquisition, a total of 15 XAS spectra were obtained. A diluted pellet of VN powder was also measured in fluorescence mode and used as a reference. The V_2O_3, VO_2 and V_2O_5 samples were measured in transmission mode, using the three ionization chambers as detectors. The energy calibration of XAS spectra, recorded in fluorescence as well in transmission mode, was assured by monitoring the glitches position of the incident beam between 5720 and 5740 eV. The energy resolution given by the Si(111) monochromator was 0.2 eV at V K-edge energy.

Determination of the specific area / projected length by AFM

AFM (Atomic Force Microscope) Dimension 3100 (Bruker) was used in intermittent contact mode with an antimony-doped Si cantilever (resistivity was 0.01 – 0.025 Ohm.cm, frequency resonance ranged from 130 to 250 kHz –with a constant stiffness k ~ 48 N/m-) in order to measure the RMS roughness and to observe the surface morphology of the VN films. Using the free software, Gwyddion, by P. Klapetek *et al*. (version 2.45, 2016) for the analysis of the AFM images, we were able to determine the projected length, Lp, of the column, i.e. the total perimeter of the columns measured by the projection of the pillar boundary on a horizontal plane (see the detailed description of the process in [2]). As the analysis of a surface could depend on its location across a 3-inch

diameter wafer, we performed 12 measurements across the wafers. Thus, all the data (roughness and L_p) are averaged out over 12 measurements, and the dispersion of the measured roughness and L_p is between 3 and 10 %, i.e. there is a good homogeneity of the sputtering process over the wafer. Considering a cylindrical shape of the columns, the specific surface area, $S_{e,}$ of the columns is deduced from L_p multiplied by the film thickness. This approach could possibly underestimate the exact value of the developed surface since the columns have an imperfect cylindrical shape, yet contain some additional 3D features. Nevertheless, this permits the determination of the S_e evolution versus the growth conditions of the film. Finally, we were able to determine the contribution of the columns terminating in a pyramidal shape (biggest ones) to L_p values.

Electrochemical analyses

The electrochemical analyses of the VN thin films were carried out by cyclic voltammetry with a VMP3 potentiostat/galvanostat (Biologic) using a conventional three-electrode setup in 1M KOH aqueous electrolyte. The reference and the counter electrodes were Hg/HgO and a platinum wire, respectively. The Si / Si_3N_4 / VN sample was assembled as the working electrode in a flat cell designed by Biologic (**figure S3B**): the sample was sandwiched between a top and a bottom cells and the sealing was ensured by O-rings. A large cavity was drilled in the top cell allowing to fill the cavity with ~1 mL of KOH electrolyte. The O-ring's diameter defines the surface test of the VN films (0.4 cm^2). VN thin films were cycled between -1 V and -0.4 V vs Hg/HgO according to the suitable conditions [3] proposed by D. Belanger *et al*. The capacitance was extracted from the CV and the surface capacitance was calculated taking into account the footprint surface delimited by the O-ring. Thanks to the high electronic conductivity of the VN layer, the films were used as a bi-functional material, thus acting both as the working electrode and the current collector. The

MSCs were characterized in 1M KOH electrolyte. Galvanostatic charge and discharge plots were investigated using the Biologic VMP3 potentiostat/galvanostat at different current densities.

In Situ AFM of VN / VN micro-supercapacitor in 1M KOH

A Bioscope AFM (Bruker) was used in intermittent contact to follow the possible expansion of VN-based MSC upon charge / discharge cycling. These *in situ* measurements were done in a home-made electrochemical cell (see the photo in **Figure SI5**), where a platinum wire was used as the counter electrode and Hg/HgO as the reference electrode. In KOH electrolyte, we used silicon nitride cantilevers working at a frequency of 5 kHz or 23 kHz with a constant stiffness of k ~ 0.6 N/m. A constant potential was applied to one of the MSC's VN electrodes for 2 minutes, and AFM imaging was performed during this period. The potential was then increased from -0.4 V down to -1 V (step = 0.2 V) vs Hg/HgO and from -1 V to -0.4 V vs Hg/HgO.

Supplementary Text

XPS analysis

Figure S2B shows the X-ray photoelectron spectroscopy survey scans performed at the surface of the VN film and in the 2nd and 3rd craters. Peaks corresponding to V *2p*, C *1s*, N *1s* and O *1s* are immediately visible on all surveys, whereas a weak contribution from Si *2p* is found in the survey spectrum for the VN / Si_3N_4 interface (3rd crater). The above observation implies that the Si_3N_4 has been reached for the 3rd crater, and that the XPS analysis was done at the VN / Si_3N_4 interface.

Figure S2C represents the evolution of the V/N and V/(O, N) total atomic ratio, determined at the surface, in the intermediate crater and at the VN / Si_3N_4 interface. The ratios were calculated from the area of V *2p*, N *1s* and O *1s* XPS spectra after a Shirley-type background subtraction.

In the case of the VN V *2p* spectra, Indlekofer *et al.* [4] reported the presence of two satellite structures on the high BE side of the V *2p* main peak, with an intensity dependent on the nitrogen content, due to poorly screened core-hole states. Here, the interpretation is rather complex due to the presence of VO_x and/or $VN_{1-x}O_x$ species because the VN satellite structures fall into the BE range for subsequent compounds. Therefore, the VN satellite features in the V *2p* spectra were omitted in the fitting as their intensities are unknown. This will effectively cause a slight overestimation of the two oxides compared to the nitride component.

The N 1s spectrum is reported in **Figure S2D**. It presents a main contribution, centered at 397.5 eV, which corresponds to V-N bonding in the vanadium nitride phase [5]. A small contribution at lower binding energy, around 396.7 eV, can be ascribed to a vanadium oxynitride phase [6], while the contributions at higher BE are consistent with NO_xC_y species. Going deeper into the film, the oxynitride shoulder at 396.7 eV becomes less intense as compared to the VN peak, until the disappearance of this contribution at the VN / Si_3N_4 interface.

TEM analysis

Different contrasts are highlighted in the TEM images of **Figure S1**: some areas are more granular (green rectangle) and some look like brighter veins (yellow rectangle). An enlargement of these zones shows small crystalline domains separated by amorphous areas. The inter-planar distances generated by the Fourier transform are compatible with the d_{111}=2.38 Å and d_{002}=2.06 Å of the face-centered cubic VN lattice (a = 4.13 Å), and confirm that the crystallized phase is VN. A careful examination of the yellow zone shows that the fringes are not correlated to the brighter contrast of the veins, which led us to attribute this latter contrast to the amorphous phase.

XRD analysis of the VN films

The structural analyses of VN thin films deposited at 100 °C as a function of the thickness is shown in **figure S5D**. The VN thin films (PDF card: 00-035-0768) are polycrystalline and seems to be strongly oriented along the [111] direction when the thickness is lower than 7 µm. As soon as the thickness is higher than 7 µm, additional Bragg peaks ((200), (220) & (311)) are observed within the diffractogramms confirming the polycrystalline nature of the VN films. Except the Bragg peak at $2\theta = 69°$ attributed to the Silicon wafer, no additional crystallized phase was identified. The intensity of this peak decreases for thicker VN films due to the constant penetration depth of the X-Ray beam in the Si / Si_3N_4 / VN stacked layers.

Electrochemical analysis as a function of the film thickness

From CV experimentation, we extracted the peak current vs the sweep rate (**Figure S6A**). It is well known that the current follows the power law ($I = av^b$), where "I" represents the current density (mA cm^{-2}) and "ν" the sweep rate (mV s^{-1}). In this formula, "a" and "b" are variable coefficients. The b-value allows for the determination of the electrochemical process type involved in charge storage within the VN films. A b-value of ~ 0.5 reflects a purely diffusion-limited process, such as reported in battery-type material and capacitive or pseudocapacitive processes leading to a b-value approaching 1. From **Figure S6B**, we observe a decrease in the b-value from 0.96 to 0.85, which indicates that the charge stored in the VN thick films arises from an electrochemical process that is not limited by solid-state diffusion when the thickness moves from 0.3 up to 16 µm.

The evolution of the surface and volumetric capacitance values vs the sweep rates is plotted in **Figures S6C** and **S6D** for all of the sputtered VN electrodes ranging from 0.3 µm up to 16 µm-thick. The CV plots of the 16-µm thick film vs the scan rates is depicted in **Figure S6E** — the low

concentration of the KOH electrolyte (1M KOH) induces a distortion of the CV at 0.1 V s^{-1}, reducing the areal capacitance (**Figure S6E**) of the 16 µm-thick film at high sweep rate (0.65 F cm^{-2}). To improve the electrochemical performance at 0.1 V s^{-1}, a more concentrated electrolyte (7M KOH) was used to evaluate the film capacitance (**Figure S6F**). While the 16 µm-thick VN film delivers the same capacitance that it does in 1M KOH (up to 1.2 F cm^{-2} at 5 mV s^{-1}), the areal capacitance remains higher than 0.9 F cm^{-2} at 0.1 V s^{-1} in 7M KOH. This finding clearly demonstrates that the electrode performance at high sweep rates is limited by the electrolyte concentration, and not by the electrode material itself.

In situ AFM on interdigitated micro-supercapacitors

The AFM test setup operating in aqueous electrolyte is illustrated in **Figure S7A**, while the top view of the MSC exhibiting two interdigitated electrodes is shown in **Figure S7B**. A dry plasma etching process compatible with CMOS technology was again used to isolate the two VN electrodes (0.325 µm depth). The fabrication process is described in the Methods section.

References for supporting text

1 V. Briois, C. La Fontaine, S. Belin, L. Barthe, T. Moreno, V. Pinty, A. Carcy, R. Girardot and E. Fonda, *J. Phys. Conf. Ser.*, 2016, **712**, 12149.

2 S. Ouendi, K. Robert, D. Stievenard, T. Brousse, P. Roussel and C. Lethien, *Energy Storage Mater.*, , DOI:10.1016/j.ensm.2019.04.006.

3 Y. Borjon-Piron, A. Morel, D. Bélanger, R. L. Porto and T. Brousse, *J. Electrochem. Soc.*, 2016, **163**, A1077–A1082.

4 G. Indlekofer, J.-M. Mariot, W. Lengauer, E. Beauprez, P. Oelhafen and C. F. Hague,

Solid State Commun., 1989, **72**, 419–423.

5 G. A. Fontalvo, C. Mitterer, N. Fateh, S. Surnev, A. Glaser and F. P. Netzer, *Surf. Sci.*, 2007, **601**, 1153–1159.

6 R. Sanjinés, C. Wiemer, P. Hones and F. Lévy, *J. Appl. Phys.*, 1998, **83**, 1396–1402.

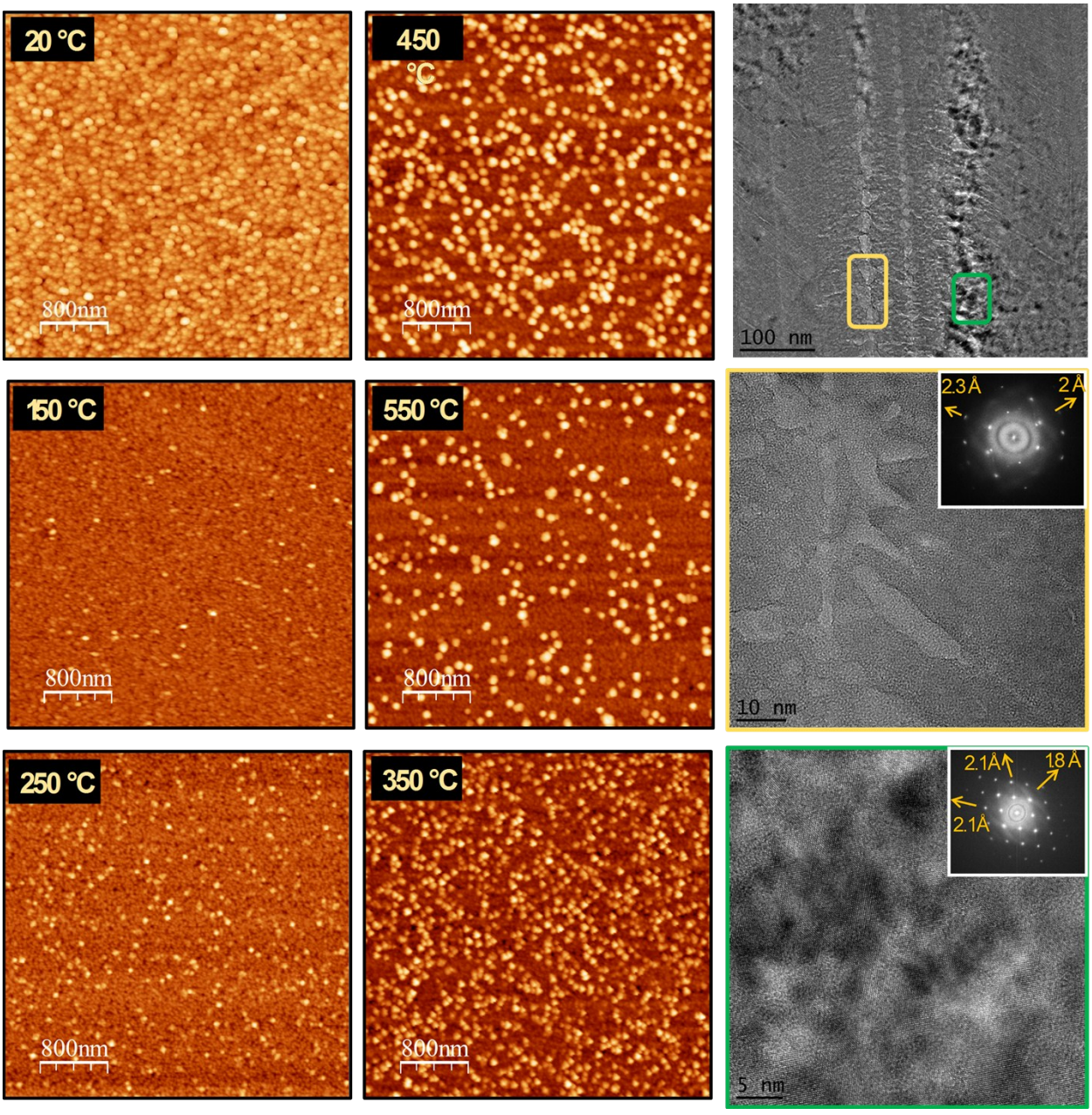

Figure S1 – AFM and TEM analyses of the VN samples. The AFM imaging was performed at various temperatures, while the TEM structural analysis was carried out on a sample deposited at 100 °C. TEM images highlighting different contrast (yellow and green rectangle). Fourier transform of the crystallized zone in this area indicate the inter-reticular distance of VN.

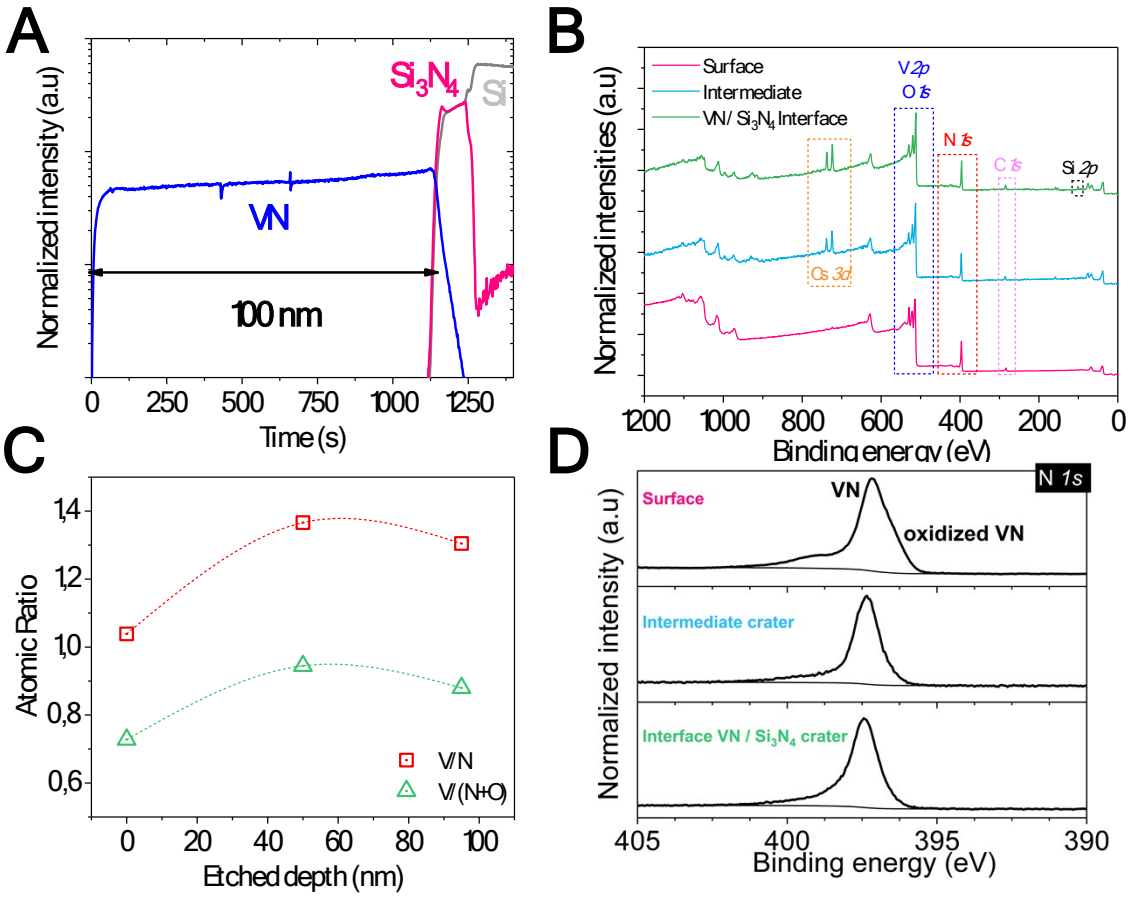

Figure S2 – **A.** TOF-SIMS profile of the vanadium, nitrogen and silicon elements in the 100 nm-thick VN sample deposited on Si_3N_4-coated Si wafer. **B.** XPS analyses (survey scan) of the 100 nm-thick VN film — the analyses are carried out at the surface, in the intermediate crater and at the VN / Si_3N_4 interface. **C.** Evolution of the atomic ratio as a function of the etched depth. **D.** N *1s* core level spectra of the vanadium nitride as a function of the etched depth.

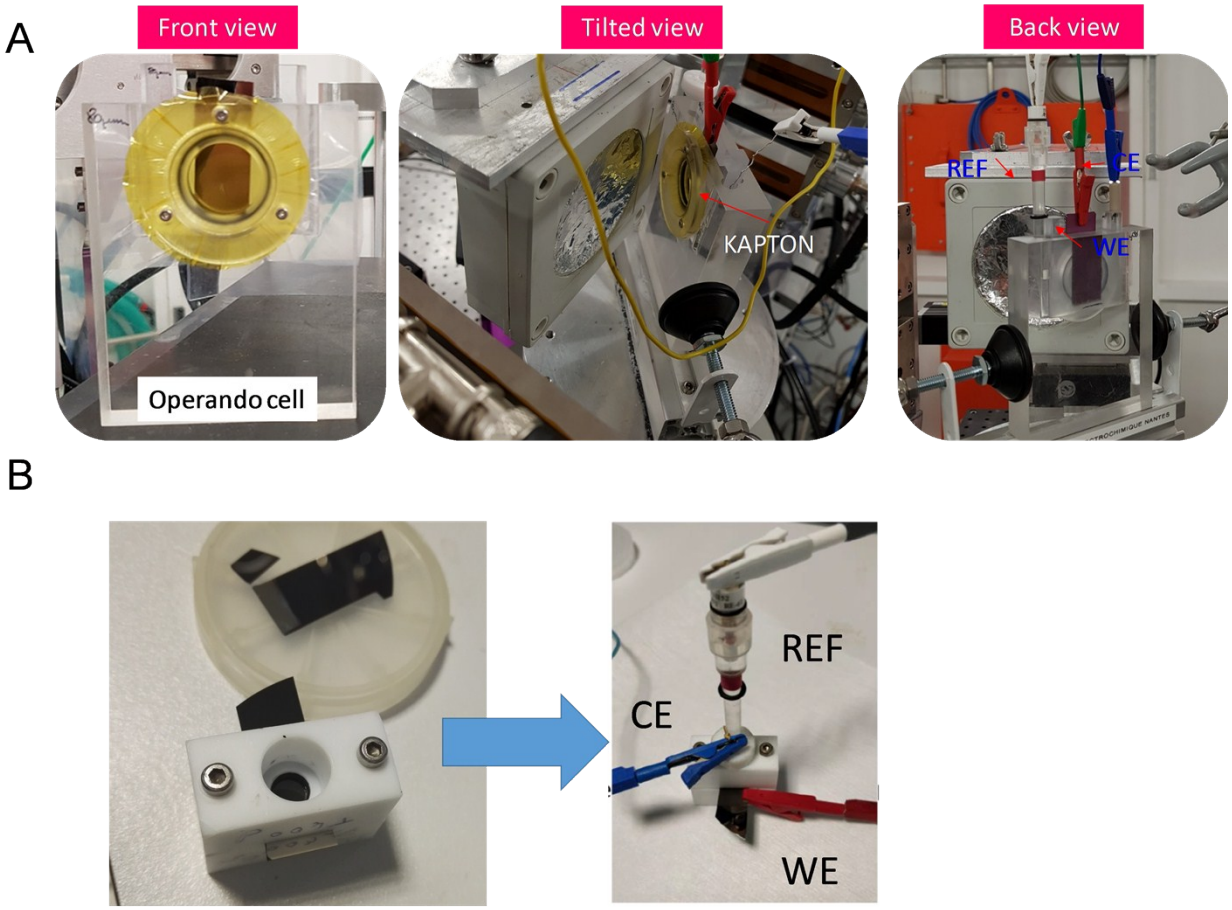

Figure S3 – **A.** Electrochemical cell used to perform the *operando* X-ray absorption spectroscopy experiments in KOH electrolyte. **B.** Electrochemical cell issued from Biologic to carry out the analysis of sputtered VN films deposited on Si substrate.

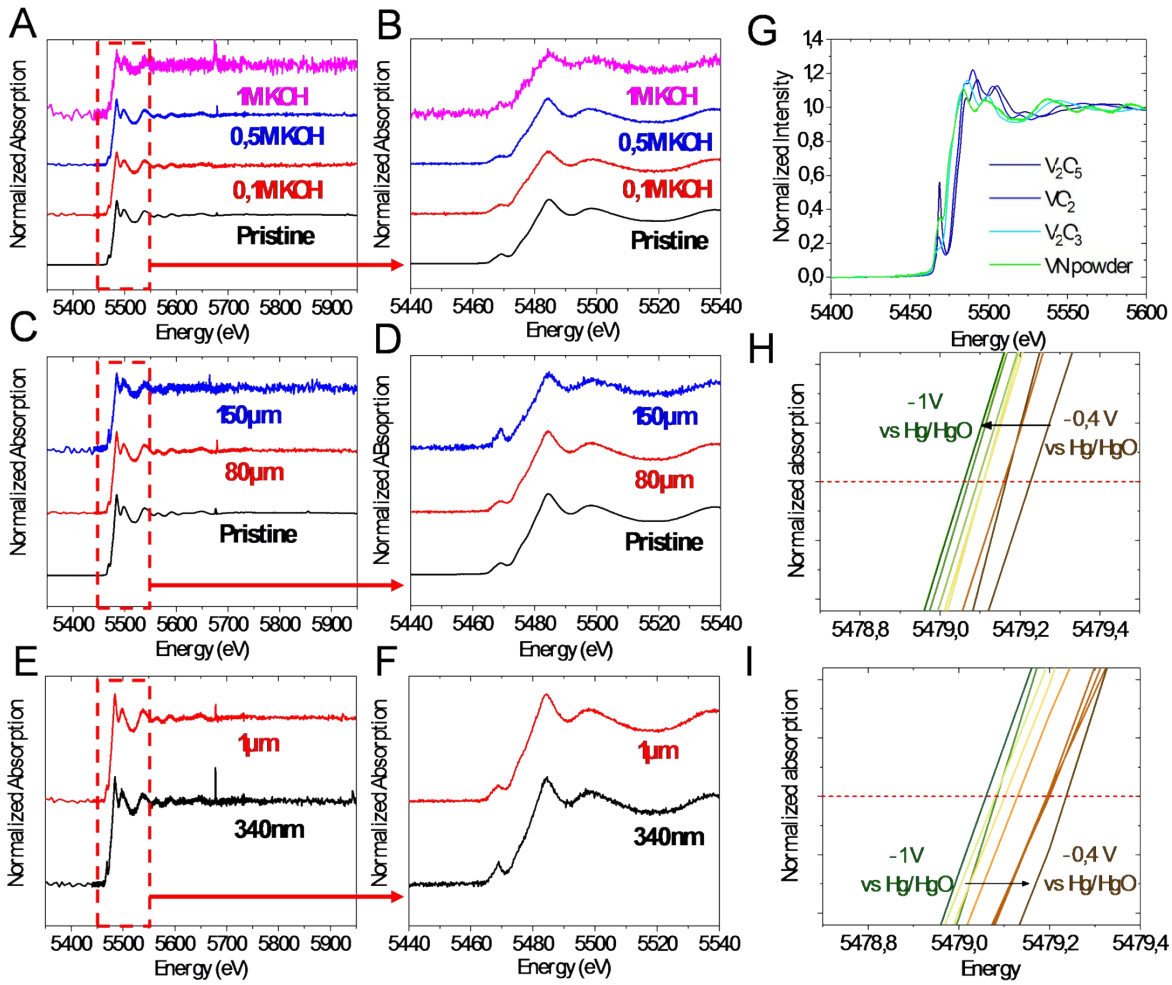

Figure S4 – XAS spectra at the V K-edge optimized as a function of the operating conditions: **A-B.** depending on the concentration of the electrolyte; **C-D** as a function of the amount of electrolyte between the incident beam of the samples; **E-F.** depending on the mount of active material. **G.** XAS spectra of the reference compounds. **H-I.** Shift of the absorption edge in 0.5M KOH electrolyte upon charge/discharge cycling.

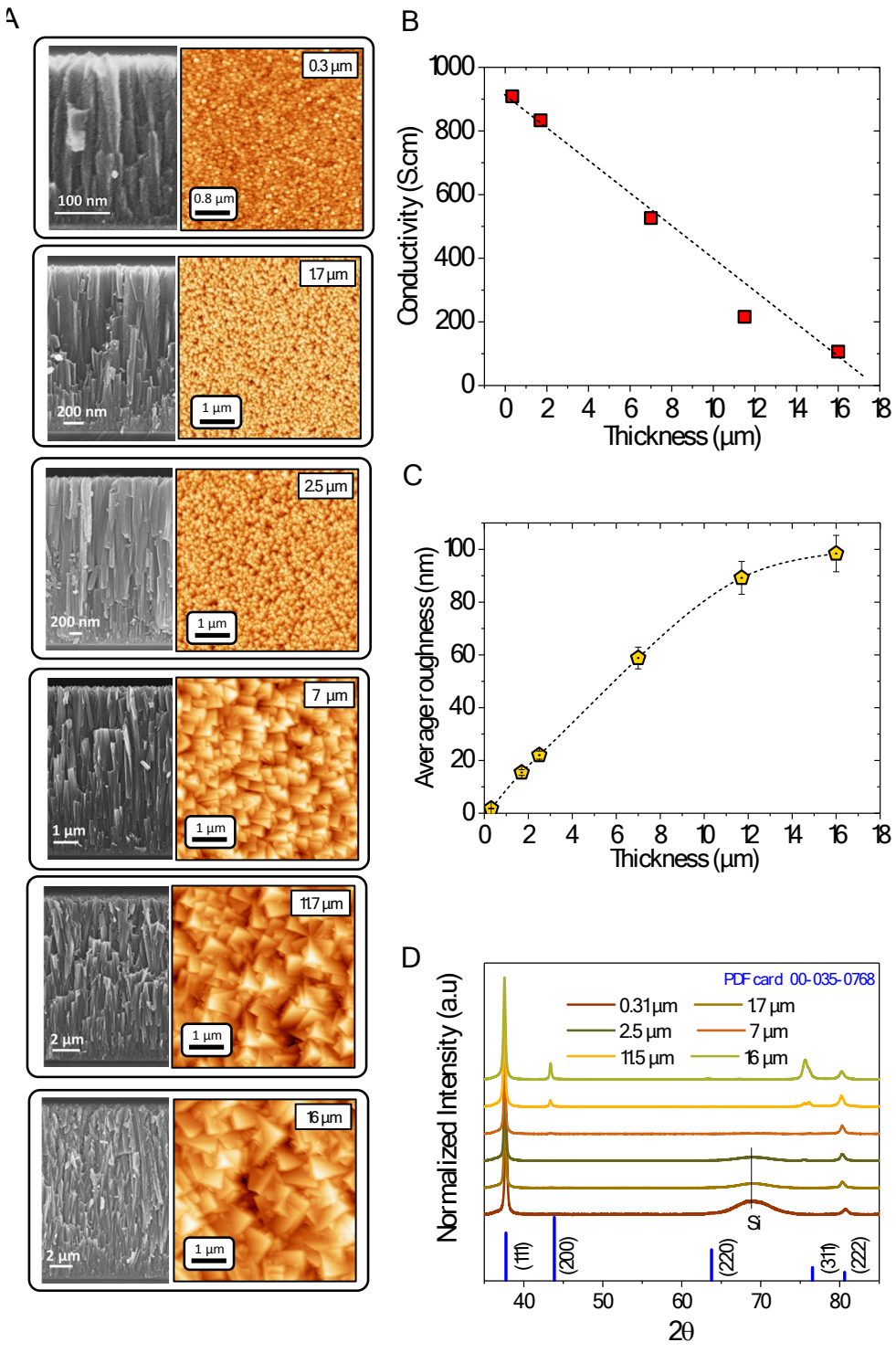

Figure S5 – **A.** SEM cross-sections and AFM top view analyses of the VN samples as a function of the film thickness. **B-C.** Evolution of the roughness and electrical conductivity of the VN films

according to their thickness. **D.** XRD analysis of the sputtered VN films as a function of the film thickness.

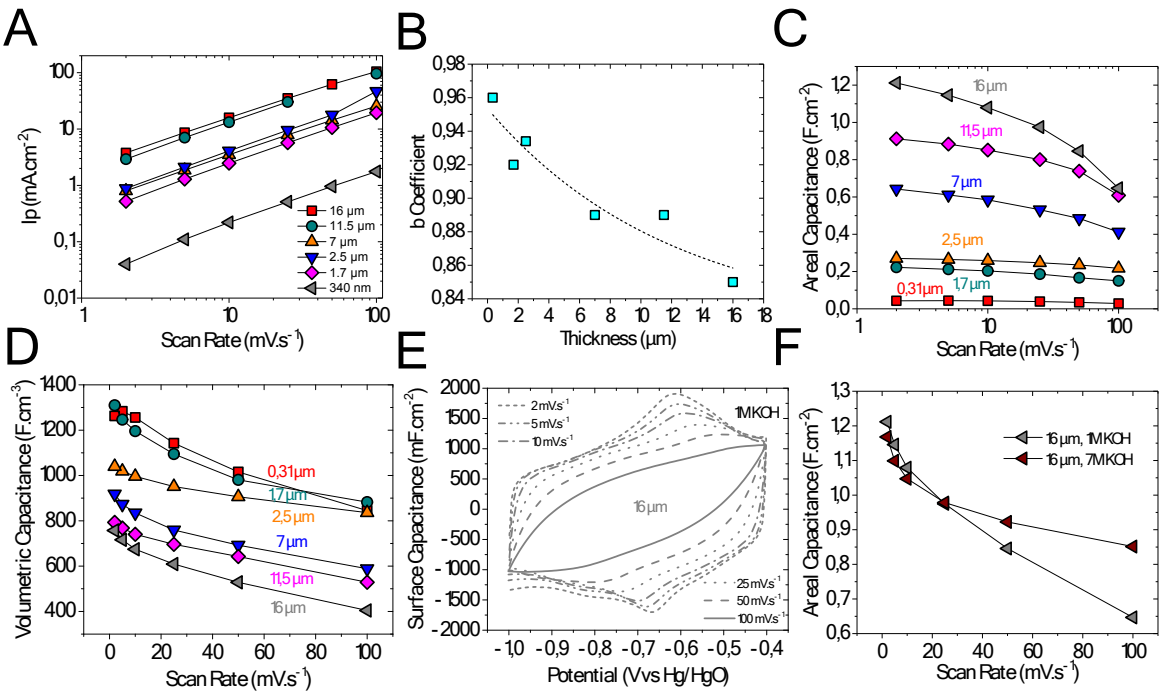

Figure S6 – Electrochemical analysis of the VN films deposited at 100 °C as a function of the thickness.

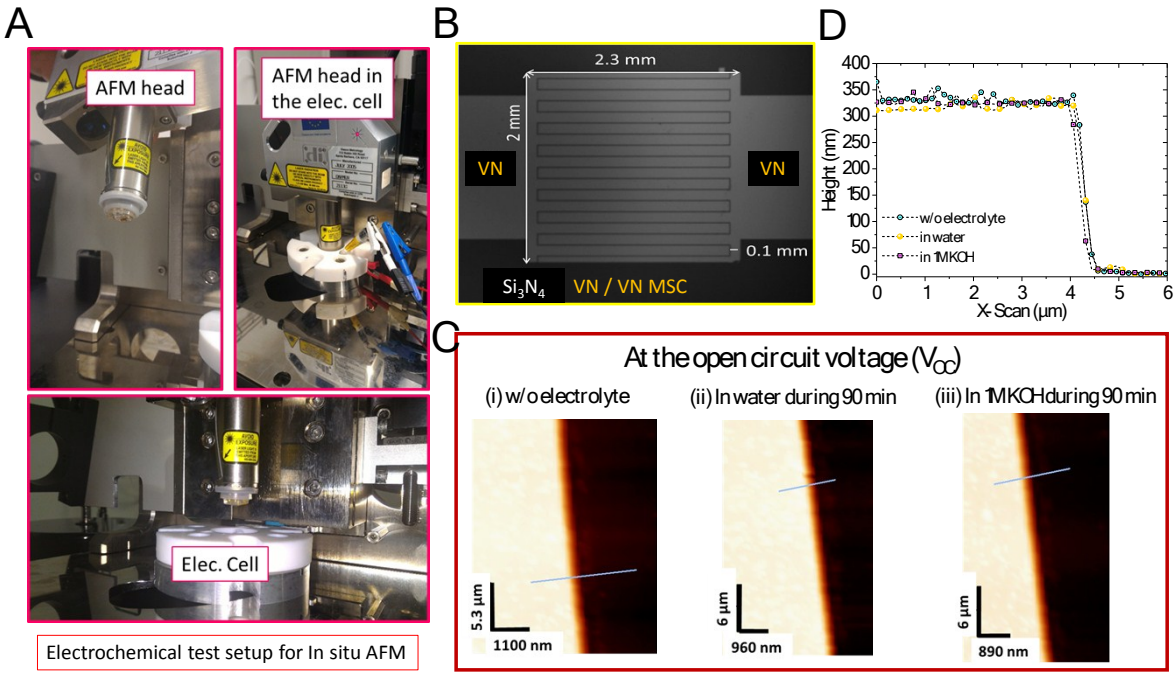

Figure S7 – A. Experimental test setup used to achieve *in situ* AFM measurements on VN / VN interdigitated MSCs. **B.** SEM top view of the interdigitated MSCs. **C-D.** The thickness of the VN electrodes is measured from cross-section AFM images and it remains constant and equal to 325 nm, in air, water or 1M KOH for 90 min, i.e. a much longer duration than the length of the voltammetric cycles, which last only a few seconds.

Movie S1.

In situ AFM of on-chip interdigitated MSCs in 1M KOH. The AFM tip scans the edge of one of the electrodes, while keeping the potential at a constant level during the scan.